A Journal of the German Chemical Society

Angewandte International Edition Chemie

GDCh

www.angewandte.org

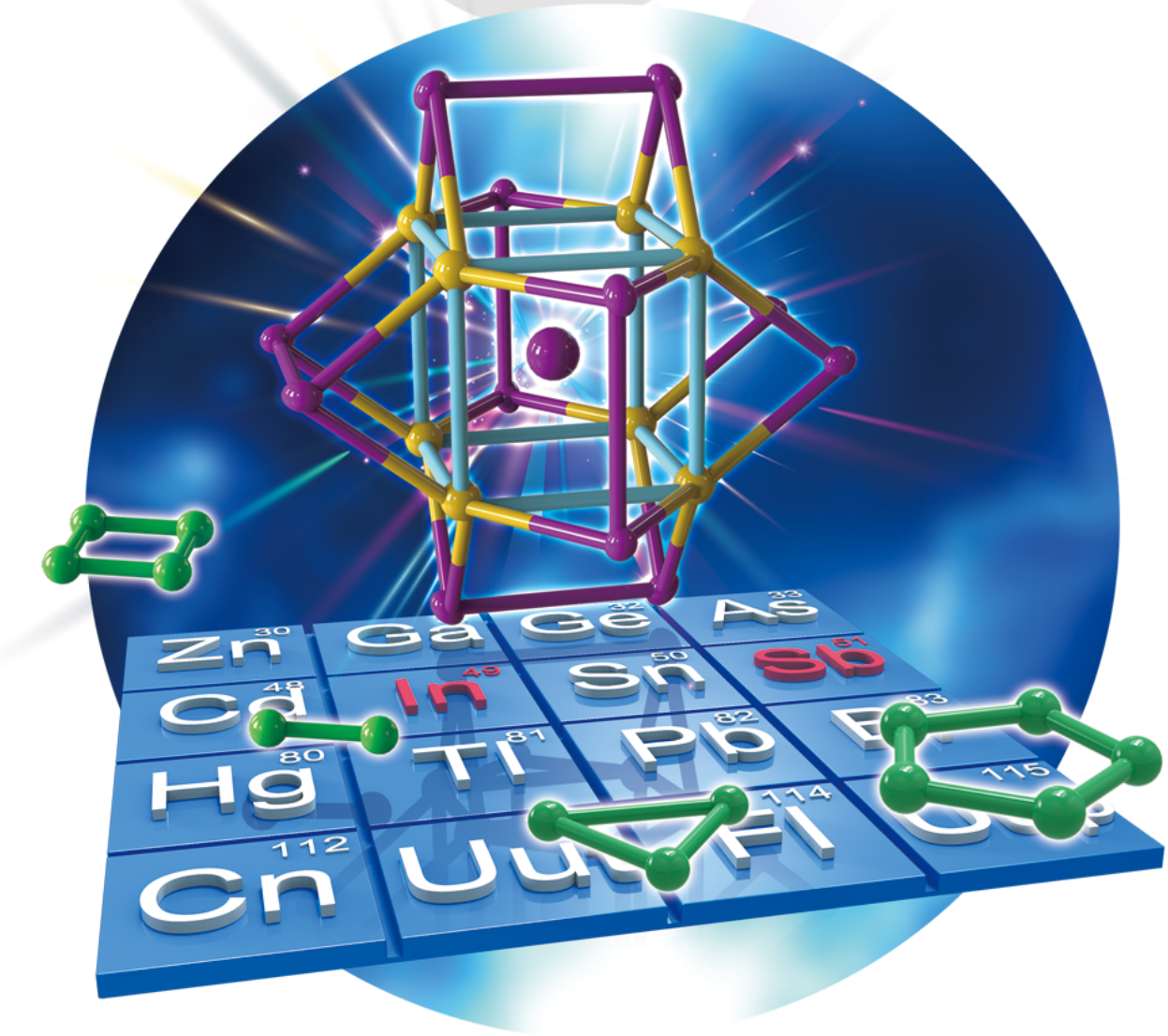

The first mixed In/Sb Zintl anion, a cluster that effectively appears as $[Sb@In_8Sb_{12}]^{4-}$, but actually is a 1:1 mixture of $[Sb@In_8Sb_{12}]^{3-}$ and $[Sb@In_8Sb_{12}]^{5-}$, has been synthesized and structurally characterized, as shown by Z. M. Sun et al. in their Communication (DOI: 10.1002/anie.201904109). The tri-anion features perfect T_h symmetry and contains eight equivalent In^{3+} centers in a cube, while in the penta-anion, the presence of two additional electrons induces a symmetry breaking, which substantially distorts the structure away from the T_h symmetry.

WILEY-VCH

Zintl Clusters

International Edition: DOI: 10.1002/anie.201904109
German Edition: DOI: 10.1002/ange.201904109

Structure and Bonding in $[Sb@In_8Sb_{12}]^{3-}$ and $[Sb@In_8Sb_{12}]^{5-}$

*Chao Liu[+], Nikolay V. Tkachenko[+], Ivan A. Popov[+], Nikita Fedik, Xue Min, Cong-Qiao Xu, Jun Li, John E. McGrady, Alexander I. Boldyrev, and Zhong-Ming Sun**

Abstract: *We report the characterization of the compound $[K([2.2.2]crypt)]_4[In_8Sb_{13}]$, which proves to contain a 1:1 mixture of $[Sb@In_8Sb_{12}]^{3-}$ and $[Sb@In_8Sb_{12}]^{5-}$. The tri-anion displays perfect T_h symmetry, the first completely inorganic molecule to do so, and contains eight equivalent In^{3+} centers in a cube. The gas-phase potential energy surface of the penta-anion has eight equivalent minima where the extra pair of electrons is localized on one In^+ center, and these minima are linked by low-lying transition states where the electron pair is delocalized over two adjacent centers. The best fit to the electron density is obtained from a model where the structure of the 5− cluster lies close to the gas-phase transition state.*

Highly symmetric nanoclusters based on regular polyhedra such as the Platonic or Archimedean solids have always held an intrinsic aesthetic appeal, but they also have intriguing chemical and physical properties.[1,2] Icosahedral (I_h) motifs are well established in coordination compounds,[3] polyoxometalates,[4] and also metalloid clusters,[5] but examples amongst free-standing inorganic clusters remain rather rare. The most prominent of these are the $[Sn_{12}]^{2-}$ and $[Pb_{12}]^{2-}$ anions that have been observed in the gas phase[6] and are stabilized by four delocalized radial π bonds and nine delocalized on-sphere σ bonds from the 5p or 6p orbitals of Sn or Pb, respectively. The ability of these clusters to accommodate metals to form endohedral clusters $[M@E_{12}]^{q-}$ (E = Sn, Pb; Figure 1) has been confirmed by X-ray crystallography[7] and photoelectron spectroscopy, and a number of computational studies have been devoted to their electronic structure.[8,9] A second classic structural type, also with icosahedral symmetry, is the (multi)-shell-like cage

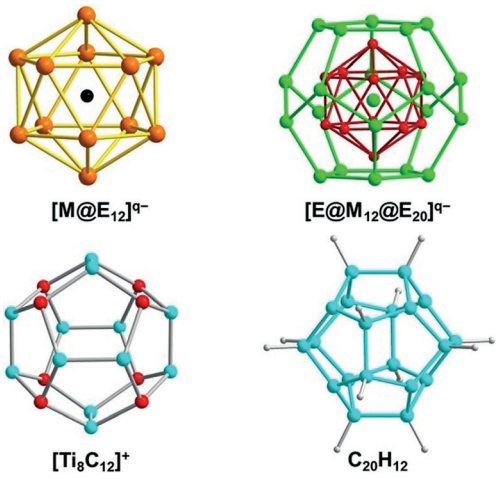

Figure 1. Structures of $[M@E_{12}]^{q-}$ and $[E@M_{12}@E_{20}]^{q-}$ with I_h symmetry, and $[Ti_8C_{12}]^+$ and $C_{20}H_{12}$ with T_h symmetry.

$[E@M_{12}@E_{20}]^{q-}$ (Figure 1), which features a centered $[E@M_{12}]$ icosahedron nested inside an $[E_{20}]$ dodecahedron. Examples from this class include $[As@Ni_{12}@As_{20}]^{3-}$,[10] $[Sb@M_{12}@Sb_{20}]^{q-}$ (M = Ni, Pd),[11] and $[Sn@Cu_{12}@Sn_{20}]^{12-}$.[12] In contrast, completely inorganic clusters with T_h symmetry have not yet been isolated in the condensed phase, although this symmetry has been proposed for the $[Ti_8C_{12}]^+$ cluster, observed as a "super-magic" peak in the mass spectra of mixtures of Ti and CH_4 or acetylene.[13] A T_h-symmetric isomer of dodecatetrahedrene, $C_{20}H_{12}$,[14] has also been the subject of computational studies, although it is substantially

[*] Dr. C. Liu,[+] Prof. Dr. Z. M. Sun
School of Materials Science and Engineering, State Key Laboratory of Elemento-Organic Chemistry, Tianjin Key Lab for Rare Earth Materials and Applications, Centre for Rare earth and inorganic functional materials, Nankai University
Tianjin 300350 (China)
E-mail: sunlab@nankai.edu.cn
Homepage: http://zhongmingsun.weebly.com/

Dr. C. Liu[+]
College of Chemistry and Chemical Engineering
Central South University
Changsha 410083, Hunan (P. R. China)

Dr. X. Min, Prof. Dr. Z. M. Sun
State Key Laboratory of Rare Earth Resource Utilization, Changchun Institute of Applied Chemistry, Chinese Academy of Sciences
5625 Renmin Street, Changchun, Jilin 130022 (China)

N. V. Tkachenko,[+] N. Fedik, Prof. Dr. A. I. Boldyrev
Department of Chemistry and Biochemistry
Utah State University
0300, Old Main Hill, Logan, Utah, 84322-0300 (USA)

Dr. I. A. Popov[+]
Theoretical Division, Los Alamos National Laboratory
Los Alamos, New Mexico 87545 (USA)

Dr. C.-Q. Xu, Prof. J. Li
Department of Chemistry and Key Laboratory of Organic, Optoelectronics & Molecular Engineering of Ministry of Education
Tsinghua University
Beijing 100084 (China)

Prof. J. E. McGrady
Department of Chemistry, University of Oxford, South Parks Road
Oxford OX1 3QZ (UK)

[+] These authors contributed equally to this work.

Supporting information and the ORCID identification number(s) for the author(s) of this article can be found under: https://doi.org/10.1002/anie.201904109.

less stable than alternative isomers with localized C=C bonds and therefore unlikely to be accessible for isolation. In this paper, we report the synthesis and characterization of an unprecedented all-metal T_h-symmetric cluster, $[Sb@In_8Sb_{12}]^{3-}$, which accommodates an Sb atom at the center of an In_8Sb_{12} cage (Figure 2). Analysis of the crystal structure, complemented by quantum-chemical calculations, shows that the highly symmetric $[Sb@In_8Sb_{12}]^{3-}$ cluster co-crystallizes with a 2-electron-reduced analogue, $[Sb@In_8Sb_{12}]^{5-}$, where the presence of an additional electron pair results in a substantial distortion away from the T_h symmetry.

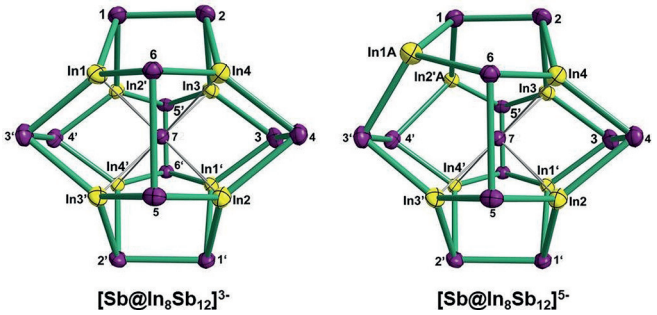

Figure 2. Structures of the $[Sb@In_8Sb_{12}]^{q-}$ core in the two components of the anionic cluster in **1**: the 5− anion contains four orientations with a summed occupancy of 0.492, only one of which is shown here.

The reaction of the Zintl phase K_5Sb_4 with In(benzyl)$_3$ at a ratio of 1:1 in ethylenediamine/toluene solvent mixtures in the presence of [2.2.2]crypt yielded crystals of $[K([2.2.2]crypt)]_4[In_8Sb_{13}]$ (**1**), in ca. 18% yield based on indium. Single-crystal X-ray diffraction reveals that **1** crystallizes in the $P\bar{1}$ space group with the anionic moiety lying on a crystallographic inversion center. The anionic moiety is a 20-vertex cage (Figure 2) that represents the first example of a binary cluster containing only In and Sb.[15] The In and Sb atoms cannot be distinguished by X-ray diffraction, but the elemental composition of the cluster was confirmed by a combination of energy-dispersive X-ray spectroscopy (EDX) analysis (Figure S6, Supporting Information) and electrospray ionization mass spectrometry (ESI-MS) (Figure S7). The EDX analysis gives an In:Sb ratio of 8.0:12.79, and the ESI-MS spectrum of single crystals of **1** dissolved in dimethylformamide (DMF), collected in negative-ion mode, reveals peaks for a dianion, $[In_8Sb_{13}]^{2-}$, with an isotope distribution almost identical to the calculated one (m/z = 1250.50; Figure 3). The diffraction data reveals a degree of disorder which only affects the positions of the eight In atoms, a possible explanation for which comes from the presence of precisely four $[K([2.2.2]crypt)]^+$ cations in the unit cell. This suggests, at first sight, that the $[Sb@In_8Sb_{12}]$ cluster carries a charge of 4− but this would imply the presence of an odd number of valence electrons. Whilst not entirely unprecedented in main-group cluster chemistry,[16] this would certainly be unusual, and we have been unable to detect any signal using electron-paramagnetic-resonance spectroscopy. An alternative possibility is that the lattice contains the

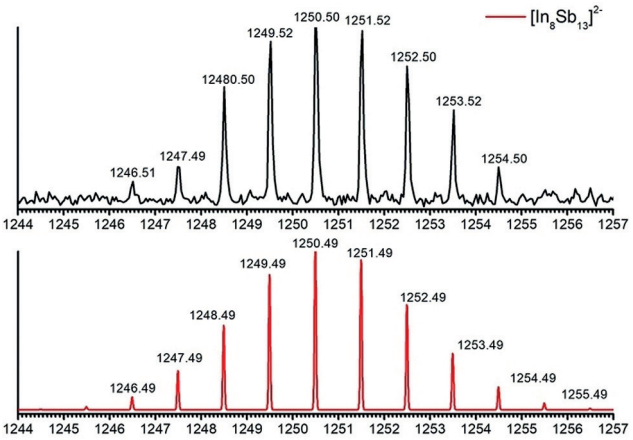

Figure 3. Negative-ion ESI mass spectrum of **1**. The spectrum shows the dianion $[Sb@In_8Sb_{12}]^{2-}$ (top) and its theoretical isotope distribution (bottom).

cluster in two distinct charge states charges, 3− and 5−, in which case structural disorder could arise from the localization of the additional two electrons at different vertices in the 5− complex. We note in this context that the co-existence of In^+ and In^{3+} in a single lattice has abundant precedent in the chemistry of the indium dihalides, InX_2 (X = Cl, Br, I), which contain In^+ and $[In^{3+}X_4]^-$.

We have tried to refine the data against a number of different models of disorder, and the best fit is achieved with a mixture of the two distinct cluster geometries shown in Figure 2 in a ratio of 51%:49%, consistent with our formulation of the crystal as a 1:1 mixture of $[Sb@In_8Sb_{12}]^{3-}$ and $[Sb@In_8Sb_{12}]^{5-}$. The first component (Figure 2, left) has a single atom at the center of a cubic arrangement of eight atoms, with a further twelve atoms arranged in pairs, capping each of the six faces of the cube (Figure S5). While a precise determination of the In/Sb atomic positions is not possible,[17] the symmetry-distinct sites in this cluster occur in the ratio 1:8:12, offering circumstantial evidence that the eight In atoms occupy the cube corner positions. If this is the case, the cluster has near-perfect T_h symmetry with four threefold axes passing through the four diagonals of the In_8 cube and three mutually perpendicular twofold axes passing through the center of each cubic face. Each In atom is coordinated to four Sb atoms in a trigonal-pyramidal geometry while the Sb atom is triply connected and pyramidal, consistent with the coordination modes observed in the intermetallic phases $A_xIn_ySb_z$ (A = Na, K).[18] The Sb–Sb contacts in the $[Sb_2]$ dimers vary between 2.812(14) and 2.847(17) Å and are comparable to those in the polystibnide Zintl clusters (2.81–2.98 Å).[19] The In–Sb distances within the $[In_8Sb_{12}]$ shell range from 2.799(6) to 2.857(12) Å with an average of 2.83 Å, comparable to the typical values in $A_xIn_ySb_z$ (2.795–3.011 Å)[18] and also in alkyl-substituted In–Sb heterocycles (2.824–2.911 Å).[20] The In–Sb bond distances in the $[Sb@In_8]$ core are slightly larger and have a relatively small dispersion from 2.977(7) to 2.995(8) Å: the coordination environment of the central Sb atom is therefore almost perfectly cubic. The In–In distances in the In_8 cube (3.433–3.476 Å) exceed the

sum of the covalent radii for a single In–In bond (2.84–2.90 Å)[21] and are longer than those found in organo-indium clusters such as $(t\text{-Bu}_3\text{Si})_6\text{In}_8$ (2.77–3.30 Å).[22] They are, however, similar to the distances in In metal itself (3.25–3.38 Å), hinting at the possibility of multicenter interactions within the [Sb@In_8] cube.

The basic structure of the second component (49%, Figure 2, right) is very similar to the first, the major difference being that one pair of mutually *cis* In vertices is displaced outwards from the center of the cluster. The overall point symmetry of the cluster is reduced to C_s, with the two In–Sb7 distances at ≈3.95 Å (average) and one almost perfectly planar Sb_3In_2 pentagon. The remaining six In–Sb7 distances remain close to 3.0 Å, almost unchanged from their values in the first component, and the Sb–Sb distances are also very similar. The disorder arises from the possibility that different pairs of mutually *cis* In vertices can be displaced outwards: the best fit to the data gives a site occupancy of 0.192 for the arrangement shown in Figure 2, right, and for its equivalent generated by inversion symmetry, as well as an occupancy of 0.054 for the corresponding structures where it is the In1A/2A pair that is displaced (Figure S2). The sum of these occupancies is 0.492, consistent with our proposal that the lattice contains a 1:1 mixture of the 3− and 5− anions.

The analysis of the crystallographic data does not, of course, establish which of the two cluster geometries corresponds to $[\text{Sb@In}_8\text{Sb}_{12}]^{3-}$ and which to $[\text{Sb@In}_8\text{Sb}_{12}]^{5-}$. Chemical intuition, however, suggests that the T_h-symmetric form is the tri-anion, made up of one Sb^{3-} anion, eight In^{3+} cations, and six $[Sb_2]^{4-}$ units. To validate this hypothesis, we have turned to density functional theory (DFT) (see the Supporting Information for details). The computed tri-anion, $[\text{Sb@In}_8\text{Sb}_{12}]^{3-}$, does indeed have a perfectly T_h-symmetric singlet ground state, with optimized Sb–Sb, In–In, and In–Sb distances within 0.07 Å of their crystallographic counterparts (see the Supporting Information). The Sb@In_8 core is slightly expanded in the DFT-optimized structure (d(In–Sb) = 3.05 Å vs. 2.98 Å from X-ray), but the major features of the structure are reproduced with encouraging accuracy. The relationship between the electron count and structure for the $[\text{Sb@In}_8\text{Sb}_{12}]^{3-}$ cluster can be appreciated most easily in a localized framework using the adaptive natural density partitioning (AdNDP)[23] algorithm as implemented in the AdNDP 2.0 code.[24] In this way, the 46 pairs of valence electrons can be partitioned into 12 s-type lone pairs on the outer Sb atoms (LPs, 1c-2e) with occupation numbers (ON) of 1.90 | e |, 6 two-center two-electron (2c-2e) Sb–Sb σ bonds, and 24 2c-2e σ bonds with ON = 1.92 | e | between the In atoms and the outer Sb centers (Figure 4). This then leaves 4 pairs of electrons in delocalized 9c-2e SbIn_8 bonds (ON = 2.00–1.97 | e |) which stabilize the In_8 cube. These four 9c-2e bonds represent linear combinations of the 5s and 5p orbitals of the central Sb atom with inwardly directed 5p orbitals on the In centers, with the major contribution coming from the central Sb atom (79.7% Sb 5s in the s-type 9c-2e bond, and 71.2% Sb 5p in each of the three *p*-type 9c-2e bonds). Therefore, the 9c-2e bonds can also be recovered as four pure LPs on the Sb atom with lower ON values, that is, 1.59 | e | for the s-type LP and 1.40 | e | for the three p-type LPs. We believe

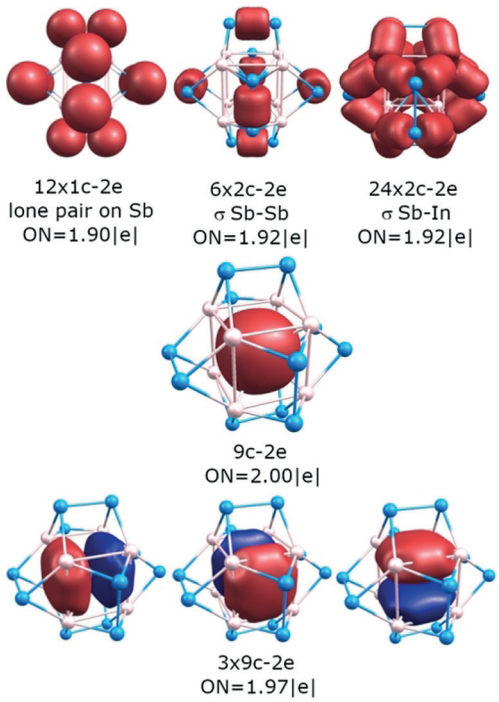

Figure 4. Bonds and occupation numbers obtained from an AdNDP analysis of the $[\text{Sb@In}_8\text{Sb}_{12}]^{3-}$ cluster. ON denotes occupation number and is equal to 2.00 | e | in the ideal case of a doubly occupied bond. Lines connecting In atoms are aids to visualization and should not be taken to represent 2c-2e bonds here and elsewhere.

that these ON values are too low, and the Sb7–In_8 interaction is therefore better described as a 9c-2e interaction. Although the cluster can be formally viewed as a neutral $\text{Sb}_{12}\text{In}_8$ unit stabilized by 2c-2e bonds between all nearest neighbors, the encapsulation of a central Sb^{3-} anion leads to a distinct contribution of the In atoms in the four SbIn_8 9c-2e bonds, that is, 2.12 | e |. This bonding model is similar to the one previously established for the 8-electron cubic silicon clusters Be@Si_8, B@Si_8^+, and C@Si_8^{2+}, where the central atom bonds to linear combinations of the sp^3-hybridized lobes of the Si atoms.[25]

The LUMO of $[\text{Sb@In}_8\text{Sb}_{12}]^{3-}$ is a three-fold degenerate, t_g-symmetric (Figure S8) linear combination of vacant p orbitals on the In centers, and therefore a perfectly T_h-symmetric singlet configuration for the penta-anion, $[\text{Sb@In}_8\text{Sb}_{12}]^{5-}$, would necessarily feature orbital degeneracy. In fact, the most stable minimum on the gas-phase potential energy surface of $[\text{Sb@In}_8\text{Sb}_{12}]^{5-}$ proves to be highly distorted, with a single In center displaced from the cubic arrangement at a In–Sb7 distance of 4.49 Å (Figure 5). The remaining seven In–Sb7 distances, in contrast, are almost unchanged at ≈3.0 Å (Figure S9, Table S2). Clearly, this structure corresponds to the localization of the additional two electrons on a single In^+ center. There are eight such minima (corresponding to the localization on each of the eight equivalent In centers), and they are connected by twelve equivalent C_s-symmetric transition states (one for each edge of the cube) where two adjacent In vertices are displaced outwards (d(In–Sb7) = 3.76 Å). The eight minima and twelve transition states

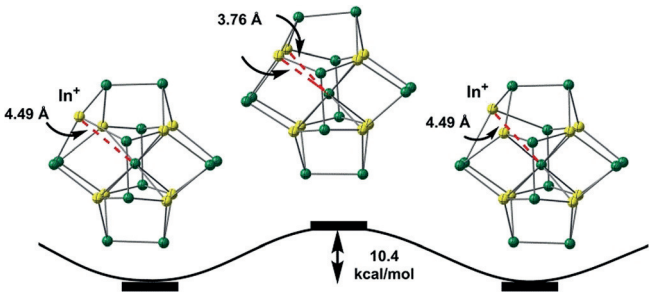

Figure 5. Gas-phase potential energy surface of the $[Sb@In_8Sb_{12}]^{5-}$ cluster.

lie around the rim of a Mexican-hat potential, and the rather low barrier of 10.4 kcal mol^{-1} indicates that the penta-anion should be highly fluxional, at least in the gas phase. The structure of the transition state is strikingly similar to the second component in the crystal structure shown in Figure 2, right: the two elongated In–Sb7 distances of 3.76 Å in the transition state compare reasonably well with the average distance of 3.95 Å that emerges from the refinement of the diffraction data. On this basis, we believe that the influence of the crystalline lattice (and, in particular, the presence of four cations) is sufficient to perturb the intrinsically flat gas-phase potential energy surface in a way that the majority of the clusters lie close to the gas-phase transition-state structure. The structural correlation model,[26] pioneered by Bürgi and Dunitz, has identified numerous examples where the crystalline environment can induce substantial distortions away from the gas-phase minimum. We note that attempts to model the electron density of the second component based on a disordered 1:1 mixture of two structures with a single displaced In center (rather than a single structure with two displaced centers) yielded an *R* factor only marginally worse than the original fit. However, the electron density can then only be reproduced if all the clusters are disordered, an observation that is incompatible with the 1:1 mixture of 3- and 5- clusters that is demanded by presence of only four cations. The analysis of C_s-$[Sb@In_8Sb_{12}]^{5-}$ using the AdNDP approach can be found in the Supporting Information (Figure S10).

In conclusion, we have synthesized and characterized the first mixed In/Sb Zintl anion, a cluster that can be formulated as "$[Sb@In_8Sb_{12}]^{4-}$", but in fact exists as a mixture of $[Sb@In_8Sb_{12}]^{3-}$ and $[Sb@In_8Sb_{12}]^{5-}$. The $[Sb@In_8Sb_{12}]^{3-}$ cluster has a cubic $Sb@In_8$ core and is almost perfectly T_h-symmetric, the first structurally characterized free-standing inorganic cluster to display such symmetry. Our analysis of the bonding in $[Sb@In_8Sb_{12}]^{3-}$ shows that it contains eight In^{3+} centers, the electron deficiency of which is partially alleviated by interaction with the s and p orbitals of the endohedral Sb center with a formally assigned charge of 3−. It is important to note that the contribution of the In atoms in the formation of the four $SbIn_8$ 9c-2e bonds is quite noticeable, that is, 2.12 | e | . Indeed, the Sb7–In_8 interactions aid in the stabilization of the In_8 cube and cannot be discounted. The endohedral structure stands in stark contrast to the binary $[Ge_4Bi_{14}]^{4-}$[27] anion that also contains two different main-group elements. It is also useful to highlight the structural relationship between $[Sb@In_8Sb_{12}]^{3-}$ and the $[Sb@M_{12}@Sb_{20}]^{q-}$ family.[11] The outer $Sb_{12}In_8$ shell can be considered topologically related to the Sb_{20} unit of $[Sb@M_{12}@Sb_{20}]^{q-}$, but the presence of a single Sb atom inside the cluster rather than an icosahedral $Sb@M_{12}$ unit pulls the eight In vertexes inwards, so that only they bond directly with the central Sb atom. The cubic coordination of Sb is also broadly consistent with the known structural chemistry of centered main-group (semi-)metal cages.[28–40] The gas-phase potential energy surface for the $[Sb@In_8Sb_{12}]^{5-}$ cluster is complex, featuring eight equivalent minima with a single displaced In^+ center, linked by low-lying transition states where the additional electron pair is delocalized over two adjacent In centers (similar to the situation found in the *trans*-bent double bonds, $R_2E{=}ER_2$, of the heavier group-IV elements). Our analysis of the X-ray data shows that the best fit for the $[Sb@In_8Sb_{12}]^{5-}$ component is a structure close to the transition state, where two In centers are simultaneously displaced outwards from the cube, rather than one or more of the minima where only a single center is displaced. Thus, it appears that the crystalline environment perturbs the gas-phase potential energy surface, so that the majority of the clusters lies close to the transition-state structure rather than the gas-phase minimum.

Experimental Section

The details of the experimental procedures, single-crystal X-ray diffraction, energy dispersive X-ray, electrospray ionization mass spectrometry, and computational methods and details are provided in the Supporting Information. CCDC 1894239 contains the supplementary crystallographic data for this paper. These data can be obtained free of charge from The Cambridge Crystallographic Data Centre.

Acknowledgements

This work was supported by the National Natural Science Foundation of China (21722106, 21571171). We also thank Prof. Jesus M. Ugalde for valuable discussions. A.I.B. gratefully acknowledges support by the USA National Science Foundation (Grant CHE-1664379). This work was supported by the US Department of Energy through the Los Alamos National Laboratory. Los Alamos National Laboratory is operated by Triad National Security, LLC, for the National Nuclear Security Administration of the U.S. Department of Energy (Contract No. 89233218CNA000001). I.A.P. acknowledges support from a Director's Postdoctoral Fellowship and J. Robert Oppenheimer Distinguished Postdoctoral Fellowship at the Los Alamos National Laboratory. C.L. acknowledges support from the Central South University Science Research Start-up Fund.

Conflict of interest

The authors declare no conflict of interest.

Keywords: Antimony · Indium · T_h symmetry · Zintl clusters

How to cite: *Angew. Chem. Int. Ed.* **2019**, *58*, 8367 – 8371
Angew. Chem. **2019**, *131*, 8455 – 8459

[1] H. W. Kroto, J. R. Heath, S. C. O'Brien, R. F. Curl, R. E. Smalley, *Nature* **1985**, *318*, 162 – 163.
[2] A. Müller, *Science* **2003**, *300*, 749 – 750.
[3] a) B. Olenyuk, J. A. Whiteford, A. Fechtenkötter, P. J. Stang, *Nature* **1999**, *398*, 796 – 799; b) S. R. Seidel, P. J. Stang, *Acc. Chem. Res.* **2002**, *35*, 972 – 983; c) J. F. Bai, A. V. Virovets, M. Scheer, *Science* **2003**, *300*, 781 – 783.
[4] a) M. Y. Gao, F. Wang, Z. G. Gu, D. X. Zhang, L. Zhang, J. Zhang, *J. Am. Chem. Soc.* **2016**, *138*, 2556 – 2559; b) A. Müller, E. Krickemeyer, H. Bögge, M. Schmidtmann, F. Peters, *Angew. Chem. Int. Ed.* **1998**, *37*, 3359 – 3363; *Angew. Chem.* **1998**, *110*, 3567 – 3571.
[5] J. Vollet, J. R. Hartig, H. Schnöckel, *Angew. Chem. Int. Ed.* **2004**, *43*, 3186 – 3189; *Angew. Chem.* **2004**, *116*, 3248 – 3252.
[6] a) L. F. Cui, X. Huang, L. M. Wang, D. Y. Zubarev, A. I. Boldyrev, J. Li, L. S. Wang, *J. Am. Chem. Soc.* **2006**, *128*, 8390 – 8391; b) L. F. Cui, X. Huang, L. M. Wang, J. Li, L. S. Wang, *J. Phys. Chem. A* **2006**, *110*, 10169 – 10172.
[7] a) E. N. Esenturk, J. Fettinger, Y. F. Lam, B. Eichhorn, *Angew. Chem. Int. Ed.* **2004**, *43*, 2132 – 2134; *Angew. Chem.* **2004**, *116*, 2184 – 2186; b) E. N. Esenturk, J. Fettinger, B. Eichhorn, *J. Am. Chem. Soc.* **2006**, *128*, 9178 – 9186; c) J. Q. Wang, S. Stegmaier, B. Wahl, T. F. Fässler, *Chem. Eur. J.* **2010**, *16*, 1793 – 1798.
[8] L. F. Cui, X. Huang, L. M. Wang, J. Li, L. S. Wang, *Angew. Chem. Int. Ed.* **2007**, *46*, 742 – 745; *Angew. Chem.* **2007**, *119*, 756 – 759.
[9] S. Neukermans, E. Janssens, Z. F. Chen, R. E. Silverans, P. von Ragué Schleyer, P. Lievens, *Phys. Rev. Lett.* **2004**, *92*, 163401 – 163401.
[10] M. J. Moses, J. C. Fettinger, B. W. Eichhorn, *Science* **2003**, *300*, 778 – 780.
[11] a) Y. Wang, M. Moses-DeBusk, L. Stevens, J. K. Hu, P. Zavalij, K. Bowen, B. I. Dunlap, E. R. Glaser, B. Eichhorn, *J. Am. Chem. Soc.* **2017**, *139*, 619 – 622; b) Z. Y. Li, H. P. Ruan, L. l. Wang, C. P. Liu, L. Xu, *Dalton Trans.* **2017**, *46*, 3453 – 3456.
[12] S. Stegmaier, T. F. Fässler, *J. Am. Chem. Soc.* **2011**, *133*, 19758 – 19768.
[13] B. C. Guo, K. P. Kerns, Jr., A. W. Castleman, *Science* **1992**, *255*, 1411 – 1413.
[14] Z. F. Chen, H. J. Jiao, A. Hirsch, P. von Ragué Schleyer, *Angew. Chem. Int. Ed.* **2002**, *41*, 4309 – 4312; *Angew. Chem.* **2002**, *114*, 4485 – 4488.
[15] C. M. Knapp, J. S. Large, N. H. Rees, J. M. Goicoechea, *Dalton Trans.* **2011**, *40*, 735 – 745.
[16] G. Espinoza-Quintero, J. C. A. Duckworth, W. K. Myers, J. E. McGrady, J. M. Goicoechea, *J. Am. Chem. Soc.* **2014**, *136*, 1210 – 1213.
[17] a) R. J. Wilson, L. Broeckaert, F. Spitzer, F. Weigend, S. Dehnen, *Angew. Chem. Int. Ed.* **2016**, *55*, 11775 – 11780; *Angew. Chem.* **2016**, *128*, 11950 – 11955; b) S. Mitzinger, L. Broeckaert, W. Massa, F. Weigend, S. Dehnen, *Nat. Commun.* **2016**, *7*, 1 – 10; c) N. Lichtenberger, N. Spang, A. Eichhöfer, S. Dehnen, *Angew. Chem. Int. Ed.* **2017**, *56*, 13253 – 13258; *Angew. Chem.* **2017**, *129*, 13436 – 13442; d) N. Lichtenberger, W. Massa, S. Dehnen, *Angew. Chem. Int. Ed.* **2019**, *58*, 3222 – 3226; *Angew. Chem.* **2019**, *131*, 3256 – 3260.
[18] W. Blase, G. Cordier, M. Somer, *Z. Kristallogr.* **1993**, *203*, 146 – 147.
[19] a) S. Scharfe, F. Kraus, S. Stegmaier, A. Schier, T. F. Fässler, *Angew. Chem. Int. Ed.* **2011**, *50*, 3630 – 3670; *Angew. Chem.* **2011**, *123*, 3712 – 3754; b) Y. Wang, P. Zavalij, B. Eichhorn, *Chem. Commun.* **2017**, *53*, 11600 – 11602; c) B. Weinert, S. Dehnen, *Struct. Bonding (Berlin)* **2017**, *174*, 99 – 134.
[20] a) A. Kuczkowski, S. Fahrenholz, S. Schulz, M. Nieger, *Organometallics* **2004**, *23*, 3615 – 3621; b) E. E. Foos, R. J. Jouet, R. L. Wells, P. S. White, *J. Organomet. Chem.* **2000**, *598*, 182 – 186.
[21] P. Pyykkö, *J. Phys. Chem. A* **2015**, *119*, 2326 – 2337.
[22] N. Wiberg, T. Blank, A. Purath, G. Stösser, H. Schnöckel, *Angew. Chem. Int. Ed.* **1999**, *38*, 2563 – 2565; *Angew. Chem.* **1999**, *111*, 2745 – 2748, and references therein.
[23] a) D. Y. Zubarev, A. I. Boldyrev, *Phys. Chem. Chem. Phys.* **2008**, *10*, 5207 – 5217; b) D. Y. Zubarev, A. I. Boldyrev, *J. Org. Chem.* **2008**, *73*, 9251 – 9258.
[24] N. V. Tkachenko, A. I. Boldyrev, *Phys. Chem. Chem. Phys.* **2019**, https://doi.org/10.1039/C9CP00379G.
[25] V. T. Ngan, M. T. Nguyen, *J. Phys. Chem. A* **2010**, *114*, 7609 – 7615.
[26] H.-B. Bürgi, *Acta Crystallogr. Sect. A* **1998**, *54*, 873 – 885.
[27] R. J. Wilson, S. Dehnen, *Angew. Chem. Int. Ed.* **2017**, *56*, 3098 – 3102; *Angew. Chem.* **2017**, *129*, 3144 – 3149.
[28] S. Scharfe, T. F. Fässler, S. Stegmaier, S. D. Hoffmann, K. Ruhland, *Chem. Eur. J.* **2008**, *14*, 4479 – 4483.
[29] E. N. Esenturk, J. Fettinger, B. Eichhorn, *Chem. Commun.* **2005**, 247 – 249.
[30] a) J. Q. Wang, S. Stegmaier, T. F. Fässler, *Angew. Chem. Int. Ed.* **2009**, *48*, 1998 – 2002; *Angew. Chem.* **2009**, *121*, 2032 – 2036; b) B. Zhou, M. S. Denning, D. L. Kays, J. M. Goicoechea, *J. Am. Chem. Soc.* **2009**, *131*, 2802 – 2803.
[31] R. J. Wilson, F. Hastreiter, K. Reiter, P. Büschelberger, R. Wolf, R. M. Gschwind, F. Weigend, S. Dehnen, *Angew. Chem. Int. Ed.* **2018**, *57*, 15359 – 15363; *Angew. Chem.* **2018**, *130*, 15585 – 15589.
[32] N. Lichtenberger, R. J. Wilson, A. R. Eulenstein, W. Massa, R. Clérac, F. Weigend, S. Dehnen, *J. Am. Chem. Soc.* **2016**, *138*, 9033 – 9036.
[33] F. Lips, R. Clérac, S. Dehnen, *Angew. Chem. Int. Ed.* **2011**, *50*, 960 – 964; *Angew. Chem.* **2011**, *123*, 991 – 995.
[34] F. Lips, M. Hołynska, R. Clérac, U. Linne, I. Schellenberg, R. Pöttgen, F. Weigend, S. Dehnen, *J. Am. Chem. Soc.* **2012**, *134*, 1181 – 1191.
[35] C. Liu, I. A. Popov, L. J. Li, N. Li, A. I. Boldyrev, Z. M. Sun, *Chem. Eur. J.* **2018**, *24*, 699 – 705.
[36] E. N. Esenturk, J. C. Fettinger, B. W. Eichhorn, *J. Am. Chem. Soc.* **2006**, *128*, 12 – 13.
[37] J. M. Goicoechea, S. C. Sevov, *J. Am. Chem. Soc.* **2005**, *127*, 7676 – 7677.
[38] Z. M. Sun, H. Xiao, J. Li, L. S. Wang, *J. Am. Chem. Soc.* **2007**, *129*, 9560 – 9561.
[39] C. Liu, X. Jin, L. J. Li, J. Xu, J. E. McGrady, Z. M. Sun, *Chem. Sci.* **2019**, *10*, 4394 – 4401.
[40] F. Lips, R. Clerac, S. Dehnen, *J. Am. Chem. Soc.* **2011**, *133*, 14168 – 14171.

Manuscript received: April 4, 2019
Accepted manuscript online: April 23, 2019
Version of record online: May 13, 2019

